

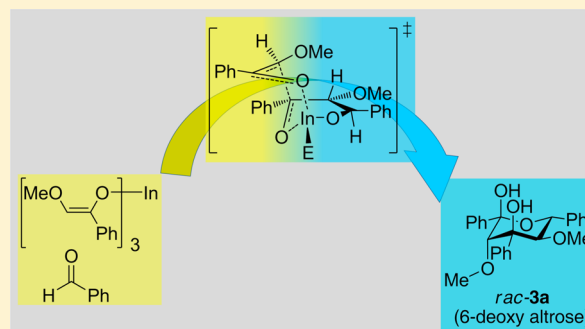
# One-Pot Domino Aldol Reaction of Indium Enolates Affording 6-Deoxy- $\alpha$ -D,L-altropyranose Derivatives: Synthesis, Mechanism, and Computational Results

M. Emin Cinar\* and Michael Schmittle\*

Department Chemie-Biologie, Universität Siegen, Adolf-Reichwein-Strasse 2, D-57068 Siegen, Germany

**S** Supporting Information

**ABSTRACT:** The domino-aldol-aldol-hemiacetal-reaction cascade of indium and other group 13 metal enolates furnished 6-deoxy- $\alpha$ -D,L-altropyranose derivatives in up to 99% yield under thermodynamic control. At lower temperature and thus under kinetic control, the reaction proceeded in a much less diastereoselective manner. The changeover from kinetic to thermodynamic control operating in this multistep domino-aldol-aldol-hemiacetal protocol was used for probing the efficiency of DFT computations. Calculations at the B3LYP/6-31G(d)/LANL2DZ level provided a mechanistic picture in full agreement with the experimental outcome.



## INTRODUCTION

Rare sugar derivatives with multiple functional groups and defined stereogenic centers are typically prepared using enzymatic protocols.<sup>1</sup> As a particular advantage, all reactions will be carried out in water and under mild conditions. In contrast, traditional carbohydrate synthesis often requires activation and protection steps putting extra stress on stereochemical control.<sup>2</sup> The aldol reaction is one of the classical methods for the formation of carbon–carbon bonds.<sup>3</sup> Metal enolates, such as those derived from titanium,<sup>4</sup> zirconium,<sup>5</sup> silicon,<sup>6</sup> and tin,<sup>7</sup> have adopted a considerable standing due to their high stereochemical control in C–C bond formation.<sup>8</sup> A similar importance can be attributed to boron enolates,<sup>9</sup> while interestingly other group 13 metal enolates have been almost completely neglected over the years.<sup>10</sup>

Despite their facile preparation, indium enolates, for example, have been sparingly used despite their proven utility in stereoselective Reformatsky<sup>10f,i</sup> and Darzens-type reactions.<sup>10f</sup> Moreover, the suggested involvement of indium enolates in indium(III)-catalyzed multistep processes, such as in the recently released tandem conjugate addition of bisenones<sup>10l</sup> and in the Conia-ene reaction,<sup>10j</sup> are encouraging to further study group 13 metal enolates in stereoselective processes.

Herein, we demonstrate that an unusual domino-aldol-aldol-hemiacetal-reaction of group 13 metals, operating best with indium, allows the fabrication of five stereogenic centers in a one-pot reaction thus opening an entry to racemic 6-deoxy altrose<sup>11</sup> derivatives (Scheme 1). The temperature dependence of product formation suggests kinetic control at 0–25 °C and thermodynamic bias at 67 °C. The suggested change from kinetic to thermodynamic control is supported by DFT computational results.

## RESULTS AND DISCUSSION

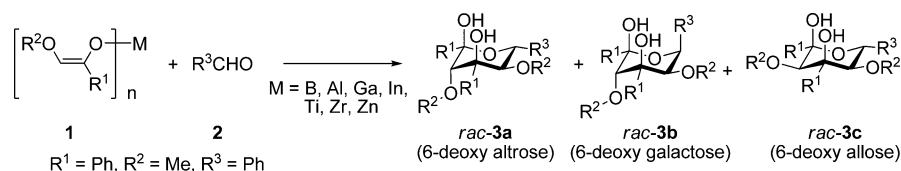
In a first set of experiments, indium enolates were prepared following a method used for the preparation of titanium bisenolates.<sup>12</sup> The indium trisenolate was generated from 2-methoxy-1-phenylethane-1-one (4) by deprotonation with lithium diisopropylamide (LDA) in dry THF and subsequent reaction with 0.33 equiv of InCl<sub>3</sub>. The resultant yellow solution was treated with a stoichiometric amount of benzaldehyde (2) and stirred for 1 h at room temperature. After aqueous workup the main product 3a was received in 43% yield (Scheme 2, with M = In<sup>12c</sup>). To better understand the mechanism and to optimize the reaction conditions, we investigated this transformation at various temperatures from –40 to 67 °C (Table 1).

At –40 °C, no aldol product of any kind was observed while at –20 °C 3a was obtained in 2% yield. With raising the temperature, the yield increased up to 99% (at 67 °C). At intermediate temperatures, though, the two diastereomeric tetrahydropyranes derivatives 3b and 3c additionally emerged. The yield of 3b first increased to a maximum of 24% at 30 °C but then dropped at higher temperatures. Similarly, the yield of 3c peaked at 25 °C with a value of 7%, but alike this diastereomer vanished at higher temperature. The monoaldol product 5 was usually received as a mixture of two diastereomers (syn/anti  $\approx$  1:1).

To identify the products, we isolated the different diastereomers via HPLC (acetonitrile/water, 3:1) and investigated their structures using NMR spectroscopic methods (Figure 1). In diastereomer 3a, characteristic NOE signals

Received: June 3, 2015

**Scheme 1.** Formation of the Protected and Functionalized 6-Deoxy- $\alpha$ -D,L-altropyranose **3a**, Galactopyranose **3b** and Allopyranose **3c** from the Reaction of Metal Enolate **1** with Aldehyde **2**



**Scheme 2.** Treatment of 2-Methoxy-1-phenylethane-1-one (**4**) with Lithium Diisopropylamide (LDA),  $\text{MCl}_3$  ( $\text{M} = \text{In}$ ) and Benzaldehyde **2** Providing **3a–c** along with Mono-Aldol Product **5**

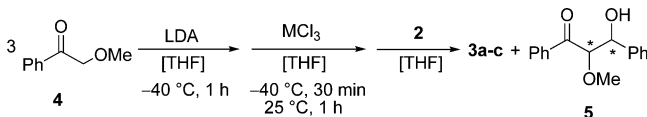


**Table 1.** Temperature Dependence of the  $\text{InCl}_3$ -Mediated Domino-Aldol-Aldol-Hemiacetal Reaction of **1** and **2** Furnishing Products **3a–3c** As Well As Mono-Aldol Product **5** (Reaction Time = 1 h)

entry	temp (°C)	yield (%)			
		3a	3b	3c	5
1	−40 <sup>a</sup>				
2	−20	2			41
3	0	11	4	2	51
4	25	43	21	7	19
5	30	53	24	4	11
6	40	57	18	3	8
7	67	99			

<sup>a</sup>Only starting material.

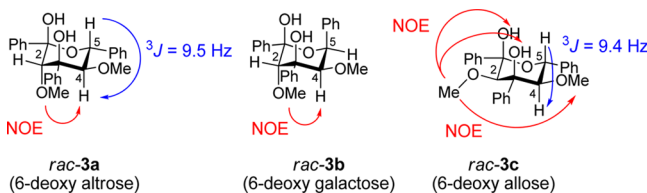


**Figure 1.** Suggested structures of **rac-3a–3c**.

showed up between the methoxy group at C2 and the ring proton 4-H (Figure 1). The combination of NOE signals and  $^1\text{H}$  NMR coupling constants ( $^3J_{4\text{-H},5\text{-H}} \sim 9.5$  Hz) indicated that in the main product **3a**, all substituents occupy equatorial positions with only the methoxy group at C2 and the two hydroxyl groups being in axial positions.

Equally in the second diastereomer **3b**, diagnostic NOE signals were detected between the methoxy group at C2 and the ring proton 4-H (Figure 1). In contrast to **3a**, no typical diaxial coupling constant was observed in the  $^1\text{H}$  NMR for the ring protons 4-H and 5-H. In summary, these results suggest that the methoxy group at C2, the phenyl group at C5 and the two hydroxyl groups are in axial positions. For the third diastereomer **3c**, a coupling constant of 9.4 Hz between the protons 4-H and 5-H was detected suggesting a diaxial arrangement. For the methoxy group at C2, an NOE revealed a close proximity to the two hydroxyl groups. These experimental results suggest that all large substituents are in equatorial positions with only the two hydroxyl groups being in

axial positions. Hence, the relative configuration of this minor diastereomer is analogous to that of the main diastereomer in domino-aldol-aldol reactions with propiophenone as an enolate component.<sup>12c</sup>

With **3a–3c** having a tetrahydro-2H-pyran-2,4-diol structure, the above reaction proceeds in a highly diastereoselective manner affording only 1 out of 16 possible diastereoisomers at 67 °C, suggesting thermodynamic control at an elevated temperature. At lower temperature, kinetic products do emerge in competition. DFT calculations at the B3LYP/6-31G(d)/LANL2DZ level indeed predict **3a** to be the most stable product at 298 K, while the relative Gibbs free energy of **3b** is 4.59 kcal mol<sup>−1</sup> and that of **3c** is 1.54 kcal mol<sup>−1</sup> higher. The computed thermodynamic stability sequence is thus in line with the exclusive formation of **3a** at 67 °C. Indirectly, this finding also suggests kinetic control at lower temperature, because the experimental diastereomeric ratio is 3:1 for **3b/3c** at 25 °C although **3b** is distinctly higher in energy than **3c** (Table 1).

The above results proposed to replace the indium salt by other group 13 metal halides. Interestingly, all reactions performed with boron(III)chloride under the optimized reaction conditions failed, while the reaction was successful with the larger  $\text{Al}^{3+}$ . For comparison, we equally conducted the reaction with titanium(IV)chloride, zirconium(IV)chloride, and zinc(II)chloride (Table 2). Although the ion radii of  $\text{Zn}^{2+}$  (74

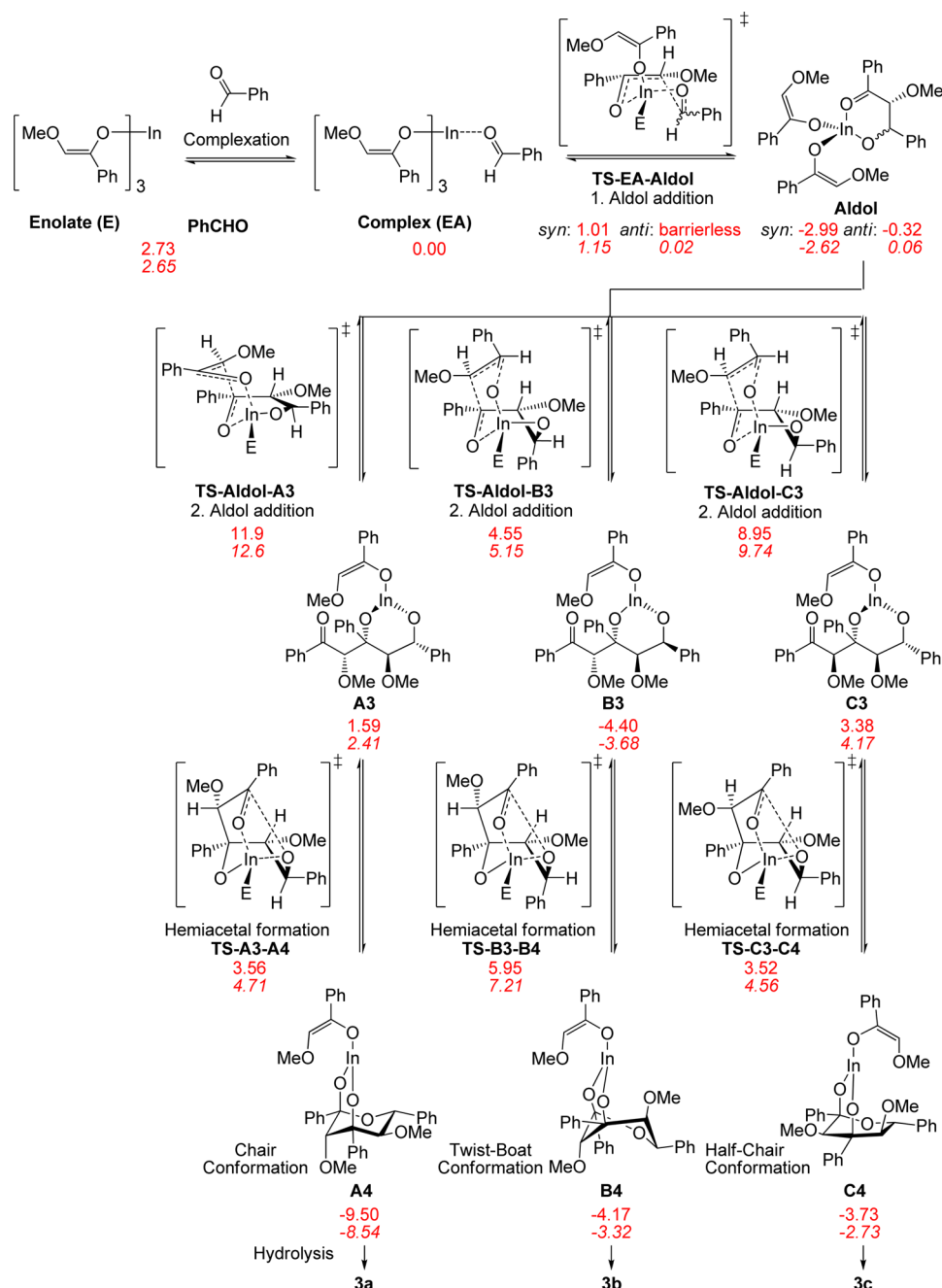
**Table 2.** Variation of the Metal Chlorides in the Domino Aldol–Aldol-Hemiacetal Reaction of **2** and **4** at 67 °C for 2.5 h<sup>a</sup>

entry	metal chloride	EN	ion-radius of metal (pm)	charge density <sup>b</sup> $z^2/r$ ( $\text{e}^2 \text{Å}^{-1}$ )	yield of <b>3a</b> (%)
1	$\text{ZnCl}_2$	1.20	74 (CN 4)	1.35	16
2	$\text{TiCl}_4$	1.30	56 (CN 4)	28.57	56
3	$\text{ZrCl}_4$	1.22	80 (CN 5)	20.0	76
4	$\text{BCl}_3$	2.01	25 (CN 4)	36.0	
5	$\text{AlCl}_3$	1.47	53 (CN 4)	16.98	52
6	$\text{InCl}_3$	1.49	76 (CN 4)	11.84	99

<sup>a</sup>EN, electronegativity by Allred and Rochow; CN, coordination number. <sup>b</sup>Charge density with respect to the coordination number.<sup>13</sup>

pm) and  $\text{In}^{3+}$  (76 pm) are comparable,  $\text{InCl}_3$  worked much better affording the product **3a** in 99% yield, which is 6 times higher than the yield obtained with  $\text{ZnCl}_2$ . On the other side, the charge density of  $\text{Zn}^{2+}$  ( $1.35 \text{ e}^2 \text{Å}^{-1}$ ) is significantly smaller than that of  $\text{In}^{3+}$  ( $11.84 \text{ e}^2 \text{Å}^{-1}$ ). A comparison of  $\text{In}^{3+}$  with  $\text{Al}^{3+}$  in terms of their ionic radii and charge densities suggests that possibly the ion radius is the dominant factor. Indeed,  $\text{Zr}^{4+}$  with a little bit larger ionic radius (80 pm) than that of  $\text{In}^{3+}$  furnished **3a** (76%) in a relatively high yield.

In brief, the domino reaction apparently follows more or less the same general pattern for  $\text{AlCl}_3$  and  $\text{InCl}_3$ . While there is no reaction with  $\text{BCl}_3$ , the yield of **3a** at 67 °C increases with the size of the group 13 metal. Most surprising is the finding that

Scheme 3. Formation of 3a, 3b, and 3c from Enolate E and Benzaldehyde (PhCHO)<sup>a</sup>

<sup>a</sup>Relative free energies ( $\Delta G_{\text{rel}}$ ) at 25 and 67 °C (in italics) with unscaled zpe computed at B3LYP/6-31G(d)/LANL2DZ level are depicted in kcal mol<sup>-1</sup> (To maintain hexa-coordination at indium,<sup>16</sup> two THF molecules were added that are not shown).

the thermodynamically most stable product 3a does exhibit the methoxy unit at C2 in an axial position.

This surprising stereochemical result and the transition from kinetic to thermodynamic control suggested challenging the power of modern DFT methods in predicting such a complex reaction scenario. Surprisingly, studies to evaluate the suitability of DFT methods for describing the reactivity of metal enolates in aldol processes are rare. There are surprisingly few reports on the aldol reactions involving boron, titanium, and tin enolates<sup>14</sup> as well as silyl enol ethers (Mukaiyama aldol<sup>15</sup>), but the present study interrogates for the first time the change between thermodynamic and kinetic control.

The results of our DFT calculations at the B3LYP/6-31G(d)/LANL2DZ level are provided in Scheme 3. Throughout the computations, we used hexa-coordination at the indium metal center,<sup>16</sup> which required filling the remaining coordination sites with THF molecules. Relative Gibbs free energies were provided at both temperatures (25 and 67 °C), which demonstrated the higher energies at 67 °C by 0.1–1.3 kcal mol<sup>-1</sup> with respect to ones at 25 °C. Nevertheless, the same trend was observed at higher temperature. Accordingly, the electrophile, i.e., benzaldehyde (2), first coordinates to the indium trisenolate E in an exergonic step ( $\Delta G = -2.7$  kcal mol<sup>-1</sup>) furnishing an enolate–aldehyde complex EA. One enolate subunit in EA reacts with the coordinated aldehyde 2

via a half-chair transition state that is energetically very low (maximum free energy of  $1.01 \text{ kcal mol}^{-1}$  relative to EA). The resulting *anti*- and *syn*-aldolates are slightly lower in energy than EA by 0.32 and  $2.99 \text{ kcal mol}^{-1}$ , respectively. The second aldol reaction of the *syn*-aldolate involves a transition state with a bicyclic half chair–boat conformation at a relative free energy of  $11.9 \text{ kcal mol}^{-1}$ . After this addition, the system flips to a half chair–chair conformation in A3 with all large substituents being now in equatorial positions except the methoxy group at C2. In the last step, the thermodynamically most stable hemiacetal A4 ( $-9.50 \text{ kcal mol}^{-1}$ ) is formed through an intramolecular cyclization via a chair–boat transition state with a relative free energy of  $3.56 \text{ kcal mol}^{-1}$  (Scheme 3). The pyranose ring in A4 has a chair conformation while the metalladioxane ring adopts a half-chair conformation. Two THF molecules bind to indium with an angle of  $82^\circ$  (O–In–O angle) thus preventing coordination of the methoxy unit at C5 with indium (Figure 2). Hydrolysis of A4 finally furnishes the domino-aldol product 3a.

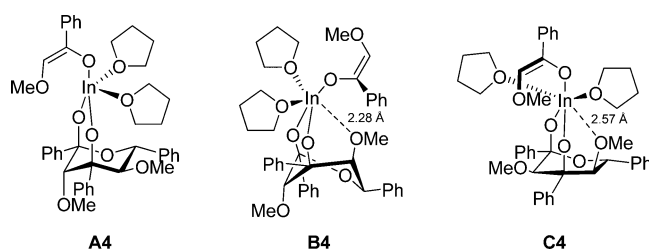


Figure 2. Structures of A4, B4, and C4 with two THF molecules.

Formation of B4, whose hydrolysis affords product 3b, requires a bicyclic transition state with a chair–boat conformation in the second aldol addition step of the *anti*-aldolate. The corresponding transition state was computed to exhibit a marginally higher energy than EA (by  $4.55 \text{ kcal mol}^{-1}$ ) furnishing B3 in an exergonic reaction. Finally, the hemiacetal formation takes place via a chair–boat transition state resulting in B4, whose relative energy is higher than that of A4 by  $5.33 \text{ kcal mol}^{-1}$  (Scheme 3). B4 exhibits a twist–boat conformation in the pyranose ring in order to avoid an axial phenyl group near the indium metal center in the chair conformation. Because of the twist–boat conformation, coordination of the MeO group with the indium center is possible ( $d = 2.28 \text{ Å}$ ) (Figure 2).

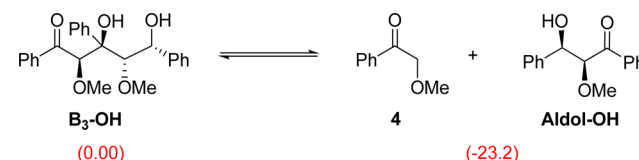
C4 with a half-chair conformation in the pyranose ring has the highest relative free energy ( $-3.73 \text{ kcal mol}^{-1}$ ) of all observed diastereomeric metal coordinated products and thus will be disfavored at higher temperature with increasing thermodynamic control. The reason for this destabilization may arise from the electrostatic interaction of the equatorial methoxy group with the indium center ( $2.57 \text{ Å}$ ) leading to a distortion of the chair conformation (Figure 2). C4 was obtained from C3 through the lowest energy transition state for hemiacetal formation ( $0.14 \text{ kcal mol}^{-1}$  with reference to C3) that is characterized by a chair–boat conformation. In contrast, formation of C3 is more endergonic than that of A3 and B3 whereas the corresponding transition state was estimated to lie between those of the other two pathways (Scheme 3).

In summary, the computational results (relative energies of A4, B4, C4, and *syn*–/*anti*-Aldol are  $-9.50$ ,  $-4.17$ ,  $-3.73$ , and  $-2.99/-0.32 \text{ kcal mol}^{-1}$ ) correctly suggest that at higher

temperature and thus under thermodynamic control, the 6-deoxy altropyranose derivative A4 and hence its hydrolysis product 3a should be preferred (Scheme 3). Moreover, the computed data rationalize the difficulty to exclusively furnish A4 at low temperature, because the formation of A3 is associated with the highest of all barriers, giving preference to the other stereoisomers as well. The computations likewise allow a rationalization of product formation under partially kinetic control (Table 1). At  $25^\circ\text{C}$ , 3a is obtained as a major product in 43% yield, whereas 3b and 3c are obtained in 21% and 7% yields, respectively. Indeed, out of the two thermodynamically disfavored products B4 and C4, formation of B4 (affording 3b after hydrolysis) has the lowest relative barrier ( $5.95$  vs  $8.95 \text{ kcal mol}^{-1}$ ). A contradiction between computations and experiment is seen though for Aldol product formation because experimentally more product 5 is found at  $25^\circ\text{C}$  (19%) than expected by computation. This finding may arise from partial hydrolysis of B3, which has almost same energy as B4, followed by a retro-aldol reaction to afford the aldol product.

To clarify the above statement, isodesmic reactions were calculated at the B3LYP/6-31G(d) level. B3-OH obtained from the hydrolysis of B3-2THF undergoes retro-aldol reaction leading to formation of Aldol-OH together with ketone 4 (see Scheme 4). The relative thermal free energies suggest the retro-aldol reaction to be a highly exergonic by  $23.2 \text{ kcal mol}^{-1}$ .

#### Scheme 4. Hydrolysis of B3-2THF May Be Followed by Retro-Aldol Reaction Furnishing the Mono-Aldol Product Aldol-OH (Free Energy in $\text{kcal mol}^{-1}$ )



To receive further insight, we tested various aldehydes in the domino reaction with the 2-methoxy-1-phenylethane-1-one (4) enolate in combination with  $\text{InCl}_3$  (1). It is interesting to see that aromatic aldehydes even containing strongly coordinating substituents (Table 3), such as the methoxy group in 7a and steric aldehydes, such as anthracene-9-carbaldehyde in 8a, are accepted in the transformation (Figure 3). While the relative configuration of 6a and 7a was readily established by  $^1\text{H}$  NMR

Table 3. Various Aldehydes in the Reaction with 2-Methoxy-1-phenylethane-1-one (4) Enolate in Combination with  $\text{InCl}_3$  (1)

entry	product	aldehyde	yield [%]
1	6a		63
2	7a		42
3	8a		74



comparison with **3a**, we ascertained the structure of **8a** by an independent NOESY experiment.

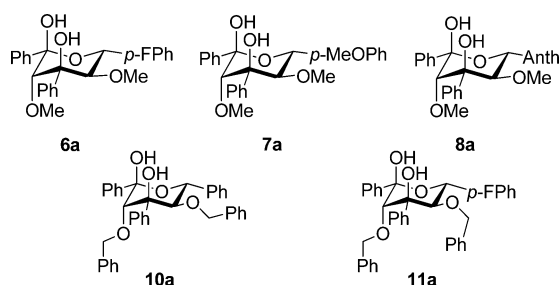
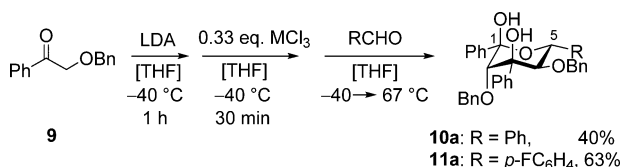


Figure 3. Structures of **6a–8a**, **10a**, and **11a**.

In further experiments, the benzyl protected 2-benzyloxy-1-phenyl-ethanone (**9**) was used opening a possibility to easily deprotect the benzyloxy groups thus providing an entry to the 6-deoxy pyranoses (see Scheme 5). Surprisingly, the expected

**Scheme 5. Reaction of Various Aldehydes with 2-Benzyloxy-1-phenyl-ethanone (**9**) in the Presence of  $\text{InCl}_3$  Leads to 6-Deoxy Altopyranoses **10a** and **11a**.<sup>a</sup>**



<sup>a</sup>4-(Dimethylamino)benzaldehyde, furfural, cinnamaldehyde, and anthracene-9-carbaldehyde did not give yield.

6-deoxy altopyranose products **10a** and **11a** were only afforded with benzaldehyde and *p*-fluorobenzaldehyde, while all other aldehydes failed to provide any of the domino-aldol-hemiacetal products (Figure 3). The reasons for this restriction are not yet clear.

## CONCLUSION

Following a domino aldol–aldol protocol, the one-pot reaction of  $\alpha$ -alkoxyacetophenones furnishes protected 6-deoxy pyranoses, mostly with the relative configuration of the 6-deoxy- $\alpha$ -D,L-altropyranose. Product formation is guided by thermodynamic control at elevated temperature affording the 6-deoxy- $\alpha$ -D,L-altropyranose as the only diastereomer and by kinetic control at reduced temperature, where up to three diastereoisomers are formed. The DFT computational results

reproduce the changeover from the thermodynamic to the kinetic control in this multistep reaction.

## EXPERIMENTAL SECTION

**General.** All reactions were carried out under an argon atmosphere by using standard Schlenk tube techniques. THF was distilled under nitrogen directly over potassium.  $^1\text{H}$ ,  $^{13}\text{C}$ , and NOESY NMR spectra were recorded on 200 and 400 MHz spectrometers, and chemical shifts were given in ppm with reference to tetramethylsilane. IR spectra were recorded on a FT-IR instrument. Elemental analyses were carried out on an elemental analyzer. Melting points are uncorrected. Compounds **3a–3c** were separated by HPLC using a reversed phase column.

**Computational Methods.** Geometry optimizations were performed at the DFT level by using the Gaussian 09 program.<sup>17</sup> Becke's three-parameter exchange functional (B3)<sup>18</sup> was employed with the Lee–Yang–Parr correlation functional (LYP)<sup>19</sup> as implemented in Gaussian 09 using Pople's split-valence 6-31G(d) basis set on C, H, O atoms and double- $\zeta$  quality basis set (LANL2DZ)<sup>20</sup> containing Hay and Wadt's effective core potential (ECP) on indium. The minima and transition states of the calculated structures were verified by analyzing the harmonic vibrational frequencies, using analytical second derivatives, which have  $\text{nimag} = 0$  and 1, respectively.

**General Procedure.** A solution of diisopropylamine (1.26 mL, 9.00 mmol) in THF (30 mL) was treated at 0 °C with 3.00 mL of *n*-butyllithium (2.5 M in *n*-hexane, 7.50 mmol) and stirred for 15 min. After cooling down to –40 °C, 2-methoxy-1-phenylethane-1-one (**4**) (1.10 mL, 7.50 mmol) was added and the mixture was stirred at –40 °C for 1 h. Then an equimolar amount of metal halide  $\text{MCl}_n$  (2.50 mmol) was added. For the experiments with titanium and zirconium, a solution of diisopropylamine (840  $\mu\text{L}$ , 6.00 mmol) in THF (30 mL) was treated with 2.00 mL of *n*-butyllithium (2.5 M in *n*-hexane, 5.00 mmol) at 0 °C and the resulting reaction mixture was stirred for 15 min. After cooling down to –40 °C (**4** (740  $\mu\text{L}$ , 5.00 mmol) was introduced and the mixture was stirred for 1 h at the same temperature. Then an equimolar amount of  $\text{MCl}_n$  (2.50 mmol) was added. For the experiments with zinc(II) salt, a solution of diisopropylamine (840  $\mu\text{L}$ , 6.00 mmol) in THF (30 mL) was treated with 2.00 mL of *n*-butyllithium (2.5 M in *n*-hexane, 5.00 mmol) at 0 °C and the reaction mixture was stirred for 15 min. After cooling down to –40 °C, 2-methoxy-1-phenylethane-1-one (740  $\mu\text{L}$ , 5.00 mmol) was injected and the mixture was stirred at –40 °C for 1 h. Afterward, it was allowed to react with an equimolar amount of metal halide (2.50 mmol).

The yellow reaction mixture of the metal enolate (with titanium red) was stirred for another 30 min at –40 °C and for 1 h at room temperature. Then, the aldehyde (2.50 mmol) in 30 mL of THF was added. After heating the mixture for 2 h at 67 °C, it was quenched with saturated aqueous  $\text{NaHCO}_3$  solution (50 mL). The aqueous layer was extracted three times with 50 mL of diethyl ether. The combined organic layers were washed with brine and dried over  $\text{Na}_2\text{SO}_4$ . The simple aldol products were characterized by comparison with literature data: *syn*-3-hydroxy-2-methoxy-1,3-diphenylpropan-1-one (*syn*-**5**).  $^1\text{H}$  NMR ( $\text{CDCl}_3$ , 200 MHz):<sup>21</sup>  $\delta$  3.26 (s, 3H), 4.64 (d,  $J = 6.1$  Hz, 1H),

Table 4. Temperature Dependence of the Domino-Aldol Reaction (7.50 mmol of **4** and 2.50 mmol of Aldehyde)

entry	temp (°C)	3a		3b		3c		5	
		mg (mmol)	%	mg (mmol)	%	mg (mmol)	%	mg (mmol)	%
1	–40 <sup>a</sup>								
2	–20	20.3(0.05)	2					263(1.03)	41
3	0	112(0.275)	11	40.7(0.100)	4	17.2(0.050)	2	327(1.28)	51
4	25	437(1.08)	43	213(0.525)	21	60.2(0.175)	7	121(0.475)	19
5	30	456(1.33)	53	207(0.600)	24	34.4(0.100)	4	70.1(0.275)	11
6	40	491(1.43)	57	155(0.450)	18	25.8(0.075)	3	51(0.200)	8
7	67	823(2.03)	99						

<sup>a</sup>Only starting material.

5.11 (d,  $J$  = 6.1 Hz, 1H), 7.20–7.60 (m, 8H), 7.88–8.00 (m, 2H); *anti*-3-hydroxy-2-methoxy-1,3-diphenylpropan-1-one (*anti*-5).  $^1\text{H}$  NMR ( $\text{CDCl}_3$ , 200 MHz):  $\delta$  3.39 (s, 3H), 4.67 (d,  $J$  = 6.6 Hz, 1H), 4.99 (d,  $J$  = 6.6 Hz, 1H), 7.22–7.62 (m, 8H), 7.86–8.05 (m, 2H).

**Effect of Temperature.** In Table 4, the yields of the products 3a–3c and 5 obtained from the domino reaction in the presence of  $\text{InCl}_3$  at different reaction temperatures are depicted.

**Effect of Metal Halides.** In Table 5, the yields of 3a using different metal halides are listed.

Table 5. Effect of Metal Halides on the Yields of 3a

entry	metal halide	3a		
		mg	mmol	%
1	zinc(II) chloride	163	0.400	15
2	titan(IV) chloride	569	1.40	56
3	zirconium(IV) chloride	774	1.90	76
4	aluminum(III) chloride	528	1.30	52
5	indium(III) chloride	1010	2.48	99

(*l,u,l*)-3,5-Dimethoxy-2,4,6-triphenyltetrahydro-2H-pyran-2,4-diol (3a). The reaction mixture containing indium(III) chloride (555 mg, 2.50 mmol) was stirred for 30 min at  $-40^\circ\text{C}$  and for 1 h at room temperature. Then, a solution of benzaldehyde (250  $\mu\text{L}$ , 2.50 mmol) in 30 mL of THF was added. The crude product was purified by crystallization from ethanol furnishing 437 mg (1.08 mmol, 43%) of 3a as a colorless solid. Mp,  $135^\circ\text{C}$ .  $^1\text{H}$  NMR (400 MHz,  $\text{CDCl}_3$ ):  $\delta$  2.36 (s, 3H), 2.49 (s, 3H), 3.47 (s, 1H), 3.60 (d,  $J$  = 12 Hz, 1H), 3.62 (s, 1H), 5.03 (d,  $J$  = 12 Hz, 1H), 6.14 (s, 1H), 7.18–7.33 (m, 9H), 7.51–7.55 (m, 4H), 7.73–7.75 (m, 2H).  $^{13}\text{C}$  NMR (100 MHz,  $\text{CDCl}_3$ ):  $\delta$  60.8, 61.7, 70.9, 79.9, 85.6, 85.8, 98.3, 125.5, 126.5, 127.5, 127.9, 128.0, 128.2, 128.3, 139.4, 141.6, 141.8. IR [KBr]: 3531, 3444, 3391, 3057, 3032, 2993, 2931, 2835, 1495, 1450, 1364, 1338, 1313, 1295, 1257, 1223, 1195, 1152, 1102, 1083, 1025, 1005, 951, 920, 874, 841, 751, 723  $\text{cm}^{-1}$ . Anal. for  $\text{C}_{25}\text{H}_{26}\text{O}_5$  (406.47 g  $\text{mol}^{-1}$ ): calcd, C 73.87, H 6.45, O 19.68; found, C 73.54, H 6.50, O 19.83.

(*l,u,l*)-3,5-Dimethoxy-2,4,6-triphenyltetrahydro-2H-pyran-2,4-diol (3b). Mp,  $128^\circ\text{C}$ .  $^1\text{H}$  NMR (400 MHz,  $\text{CDCl}_3$ ):  $\delta$  2.32 (s, 3H), 2.74 (s, 3H), 3.26 (s, 1H), 4.23 (s, 1H), 4.31 (s, 1H), 5.65 (s, 1H), 5.66 (s, 1H), 7.26–7.47 (m, 9H), 7.56 (d,  $J$  = 7.4 Hz, 2H), 7.64 (d,  $J$  = 9.4 Hz, 2H), 7.94 (d,  $J$  = 7.2 Hz, 2H).  $^{13}\text{C}$  NMR (100 MHz,  $\text{CDCl}_3$ ):  $\delta$  61.0, 61.36, 70.0, 78.5, 80.2, 87.4, 98.9, 126.3, 126.6, 126.8, 127.1, 127.4, 127.8 (2C), 128.0, 128.2, 138.5, 142.1, 142.7. IR [KBr]: 3435, 3090, 3060, 3030, 2930, 2830, 1965, 1496, 1450, 1412, 1345, 1315, 1234, 1194, 1122, 1087, 1064, 1029, 1004, 951, 926, 906, 874, 856, 841, 759, 703  $\text{cm}^{-1}$ . Anal. for  $\text{C}_{25}\text{H}_{26}\text{O}_5$  (406.47 g  $\text{mol}^{-1}$ ): calcd, C 73.87, H 6.45; found, C 73.64, H 6.72.

(*u,l,l*)-3,5-Dimethoxy-2,4,6-triphenyltetrahydro-2H-pyran-2,4-diol (3c). Mp,  $118^\circ\text{C}$ .  $^1\text{H}$  NMR (400 MHz,  $\text{CDCl}_3$ ):  $\delta$  2.16 (s, 3H), 2.74 (s, 3H), 3.15 (s, 1H), 3.89 (s, 1H), 4.14 (d,  $J$  = 9.4 Hz, 1H), 5.13 (d,  $J$  = 9.4 Hz, 1H), 6.62 (s, 1H), 7.28–7.46 (m, 9H), 7.59–7.71 (m, 4H), 7.78 (d,  $J$  = 7.2 Hz, 2H).  $^{13}\text{C}$  NMR (100 MHz,  $\text{CDCl}_3$ ):  $\delta$  60.5, 60.6, 71.6, 78.6, 80.4, 85.5, 98.4, 126.8 (2C), 126.9 (2C), 127.4, 127.6, 127.8, 128.0, 128.2, 139.9, 141.2, 141.9. IR [KBr]: 3512, 3090, 3061, 3033, 2930, 2830, 2246, 1954, 1496, 1449, 1422, 1296, 1259, 1227, 1197, 1141, 1098, 1082, 1064, 1040, 1025, 1005, 995, 978, 939, 911, 779, 752, 701  $\text{cm}^{-1}$ . Anal. for  $\text{C}_{25}\text{H}_{26}\text{O}_5$  (406.47 g  $\text{mol}^{-1}$ ): calcd, C 73.87, H 6.45; found, C 73.54, H 6.50.

(*l,u,l*)-6-(4-Fluorophenyl)-3,5-dimethoxy-2,4-diphenyltetrahydro-2H-pyran-2,4-diol (6a). The use of  $\text{InCl}_3$  (555 mg, 2.50 mmol) and 4-fluorobenzaldehyde (260  $\mu\text{L}$ , 2.50 mmol) resulted in 669 mg (1.58 mmol, 63%) of 6a as a colorless solid after crystallization from ethanol. Mp,  $153^\circ\text{C}$ .  $^1\text{H}$  NMR (200 MHz,  $\text{CDCl}_3$ ):  $\delta$  2.44 (s, 3H), 2.56 (s, 3H), 3.56 (s, 1H), 3.68 (d,  $J$  = 9.5 Hz, 1H), 3.86 (s, 1H), 5.13 (d,  $J$  = 9.5 Hz, 1H), 6.30 (s, 1H), 7.31–7.42 (m, 8H), 7.59–7.64 (m, 4H), 7.81–7.86 (m, 2H).  $^{13}\text{C}$  NMR (100 MHz,  $\text{CDCl}_3$ ):  $\delta$  60.9, 61.7, 70.2, 79.9, 85.6, 85.9, 98.4, 115.1 (d,  $J$  = 21 Hz), 125.4, 126.5, 127.6, 127.9, 128.2, 128.3, 129.1 (d,  $J$  = 8.2 Hz), 135.2, 141.5, 141.7, 161.3. IR [KBr]: 3431, 3061, 2932, 2831, 1606, 1510, 1450, 1367, 1295, 1260,

1224, 1193, 1156, 1109, 1088, 1023, 1004, 967, 953, 919, 882, 840, 806, 778, 757, 723, 700, 628  $\text{cm}^{-1}$ . Anal. for  $\text{C}_{25}\text{H}_{25}\text{FO}_5$  (424.46 g  $\text{mol}^{-1}$ ): Calcd, C 70.74, H 5.94, O 18.85; found, C 70.53, H 5.85, O 18.94.

(*l,u,l*)-3,5-Dimethoxy-6-(4-methoxyphenyl)-2,4-diphenyltetrahydro-2H-pyran-2,4-diol (7a).  $\text{InCl}_3$  (555 mg, 2.50 mmol) and 4-methoxybenzaldehyde (300  $\mu\text{L}$ , 2.50 mmol) provided 458 mg (1.05 mmol, 42%) of 7a as a colorless solid after recrystallization of crude product from ethanol. Mp,  $151^\circ\text{C}$ .  $^1\text{H}$  NMR (400 MHz,  $\text{CDCl}_3$ ):  $\delta$  2.44 (s, 3H), 2.59 (s, 3H), 3.54 (s, 1H), 3.66 (d,  $J$  = 9.2 Hz, 1H), 3.67 (s, 1H), 3.81 (s, 3H), 5.06 (d,  $J$  = 9.6 Hz, 1H), 6.21 (s, 1H), 6.93 (d,  $J$  = 8.8 Hz, 2H), 7.27–7.41 (m, 6H), 7.51 (d,  $J$  = 8.4 Hz, 2H), 7.61–7.63 (m, 2H), 7.79–7.83 (m, 2H).  $^{13}\text{C}$  NMR (100 MHz,  $\text{CDCl}_3$ ):  $\delta$  55.2, 60.8, 61.7, 70.5, 79.9, 85.6, 85.7, 98.3, 113.4, 125.5, 126.5, 127.5, 127.9, 128.1, 128.3, 128.7, 131.5, 141.7, 141.9, 159.4. IR [KBr]: 3431, 3061, 2932, 2831, 1606, 1510, 1450, 1367, 1295, 1260, 1224, 1193, 1156, 1109, 1088, 1023, 1004, 967, 953, 919, 882, 840, 806, 778, 757, 723, 700, 628  $\text{cm}^{-1}$ . Anal. for  $\text{C}_{26}\text{H}_{28}\text{O}_6$  (436.50 g  $\text{mol}^{-1}$ ): Calcd, C 71.54, H 6.47, O 21.99; found, C 71.50, H 6.43, O 21.78.

(*l,u,l*)-6-(Anthracen-9-yl)-3,5-dimethoxy-2,4-diphenyltetrahydro-2H-pyran-2,4-diol (8a).  $\text{InCl}_3$  (555 mg, 2.50 mmol) and 9-anthracenylcarbaldehyde (524 mg, 2.50 mmol) furnished 937 mg (1.85 mmol, 74%) of 8a as a colorless solid after two times crystallization from ethanol. Mp,  $172^\circ\text{C}$ .  $^1\text{H}$  NMR (400 MHz,  $\text{CDCl}_3$ ):  $\delta$  2.17 (s, 3H), 2.53 (s, 3H), 3.83 (s, 1H), 4.01 (s, 1H), 4.81 (d,  $J$  = 10 Hz, 1H), 6.67 (s, 1H), 6.81 (d,  $J$  = 10 Hz, 1H), 7.29–7.58 (m, 10H), 7.79–7.89 (m, 3H), 7.80–8.10 (m, 2H), 8.31–8.33 (m, 1H), 8.48 (s, 1H), 8.55 (d,  $J$  = 9.2 Hz, 1H), 9.20 (d,  $J$  = 9.2 Hz, 1H).  $^{13}\text{C}$  NMR (100 MHz,  $\text{CDCl}_3$ ):  $\delta$  60.2, 61.8, 66.6, 80.4, 83.3, 86.0, 99.0, 124.2, 124.6, 125.4, 125.5, 126.2, 126.3, 126.6, 127.0, 127.2, 128.0, 128.2, 128.4, 128.9, 129.1, 130.0, 130.4, 131.4, 131.7, 132.0, 134.1, 141.7, 141.9. IR [KBr]: 3544, 3456, 3062, 2989, 2932, 2829, 1676, 1624, 1592, 1527, 1494, 1447, 1404, 1333, 1251, 1158, 1104, 1026, 996, 890, 763, 728, 705, 630  $\text{cm}^{-1}$ . Anal. for  $\text{C}_{33}\text{H}_{30}\text{O}_5$  (506.59 g  $\text{mol}^{-1}$ ): Calcd, C 78.24, H 5.97, O 15.79; found, C 78.00, H 6.03, O 15.63.

(*l,u,l*)-3,5-Bis(benzyloxy)-2,4,6-triphenyltetrahydro-2H-pyran-2,4-diol (10a). A mixture of 1.70 g (7.50 mmol) of 2-benzyloxy-1-phenylethanone (9) and  $\text{InCl}_3$  (555 mg, 2.50 mmol) was treated with a solution of benzaldehyde (250  $\mu\text{L}$ , 2.50 mmol) in THF (30 mL) under reflux conditions for 2 h. The crude product was purified by crystallization from ethanol furnishing 558 mg (1.00 mmol, 40%) of 10a as a colorless solid. Mp,  $148^\circ\text{C}$ .  $^1\text{H}$  NMR ( $\text{CDCl}_3$ , 400 MHz):  $\delta$  3.35 (d,  $J$  = 10 Hz, 1H), 3.47 (d,  $J$  = 10 Hz, 1H), 3.53 (d,  $J$  = 12 Hz, 1H), 3.55 (d,  $J$  = 12 Hz, 1H), 3.68 (d,  $J$  = 1.0 Hz, 1H), 3.91 (d,  $J$  = 1.0 Hz, 1H), 4.01 (d,  $J$  = 9.6 Hz, 1H), 5.22 (d,  $J$  = 9.6 Hz, 1H), 6.43 (s, 1H), 6.50–6.55 (m, 4H), 7.04–7.20 (m, 6H), 7.36–7.45 (m, 9H), 7.63–7.66 (m, 4H), 7.87–7.89 (m, 2H).  $^{13}\text{C}$  NMR (100 MHz,  $\text{CDCl}_3$ ):  $\delta$  71.1, 74.9, 75.4, 80.3, 83.3, 84.1, 98.6, 126.8, 127.6, 127.7, 127.8, 127.9, 128.0, 128.1, 128.2, 128.3, 128.4, 128.5, 128.6, 136.4, 136.6, 139.3, 141.8, 141.9. IR [KBr]: 3089, 3080, 3059, 2978, 2927, 2870, 2760, 2720, 2488, 1954, 1816, 1602, 1586, 1497, 1453, 1397, 1358, 1334, 1315, 1294, 1256, 1224, 1155, 1091, 1077, 1013, 917, 752, 697  $\text{cm}^{-1}$ . Anal. for  $\text{C}_{37}\text{H}_{34}\text{O}_5$  (558.66 g  $\text{mol}^{-1}$ ): Calcd, C 79.55, H 6.13; found, C 79.78, H 6.43.

(*l,u,l*)-3,5-Bis(benzyloxy)-6-(4-fluorophenyl)-2,4-diphenyltetrahydro-2H-pyran-2,4-diol (11a). A mixture of 1.70 g (7.50 mmol) of 2-benzyloxy-1-phenylethanone (9) and  $\text{InCl}_3$  (555 mg, 2.50 mmol) was reacted with a solution of 4-fluorobenzaldehyde (260  $\mu\text{L}$ , 2.50 mmol) in THF (30 mL) under reflux conditions for 2 h. The crude product was purified by crystallization from ethanol providing 908 mg (1.57 mmol, 63%) of 11a as a colorless solid. Mp,  $158^\circ\text{C}$ .  $^1\text{H}$  NMR (200 MHz,  $\text{CDCl}_3$ ):  $\delta$  3.34 (d,  $J$  = 10 Hz, 1H), 3.47 (d,  $J$  = 10 Hz, 1H), 3.52 (d,  $J$  = 4.0 Hz, 2H), 3.69 (s, 1H), 3.91 (s, 1H), 4.00 (d,  $J$  = 9.6 Hz, 1H), 5.21 (d,  $J$  = 9.6 Hz, 1H), 6.42 (s, 1H), 6.48–6.56 (m, 4H), 7.05–7.15 (m, 5H), 7.32–7.47 (m, 9H), 7.60–7.66 (m, 4H), 7.85–7.89 (m, 2H).  $^{13}\text{C}$  NMR (100 MHz,  $\text{CDCl}_3$ ):  $\delta$  70.5, 74.9, 75.5, 80.3, 83.2, 84.0, 98.6, 115.1, 115.3, 126.7, 127.6, 127.8, 127.9, 128.0 (2C), 128.1, 128.4, 128.5, 128.6, 129.4, 129.5, 135.1, 136.2, 136.5, 141.6, 141.7, 161.4. IR [KBr]: 3462, 3063, 3029, 2905, 2859, 1894,

1604, 1510, 1497, 1452, 1401, 1335, 1315, 1296, 1257, 1222, 1154, 1078, 1068, 1013, 841, 805, 777, 701, 676 cm<sup>-1</sup>. Anal. for C<sub>37</sub>H<sub>33</sub>FO<sub>3</sub> (576.65 g mol<sup>-1</sup>): Calcd, C 77.06, H 5.77; found, C 77.39, H 5.99.

## ■ ASSOCIATED CONTENT

### ■ Supporting Information

The Supporting Information is available free of charge on the ACS Publications website at DOI: 10.1021/acs.joc.5b01256.

<sup>1</sup>H and <sup>13</sup>C NMR spectra, and Cartesian coordinates (computed) including the structures of all molecules (PDF)

## ■ AUTHOR INFORMATION

### Corresponding Authors

\*E-mail: schmittel@chemie.uni-siegen.de.

\*E-mail: emin.cinar@uni-siegen.de.

### Notes

The authors declare no competing financial interest.

## ■ ACKNOWLEDGMENTS

Financial support from the DFG is gratefully acknowledged. We thank Dr. Thomas Koy for valuable preparative work and helpful discussions in the early stage of this manuscript. We are indebted to the High-Performance-Computing (HPC) Linux Cluster HorUS of the University of Siegen for computational resources.

## ■ REFERENCES

- (1) (a) Brovetto, M.; Gaménara, D.; Méndez, P. S.; Seoane, G. A. *Chem. Rev.* **2011**, *111*, 4346–4403. (b) Czarnecki, P.; Plutecka, A.; Gawroński, J.; Kacprzak, K. *Green Chem.* **2011**, *13*, 1280–1287. (c) Barnard-Britson, S.; Chi, X.; Nonaka, K.; Spork, A. P.; Tibrewal, N.; Goswami, A.; Pahari, P.; Ducho, C.; Rohr, J.; Van Lanen, S. G. *J. Am. Chem. Soc.* **2012**, *134*, 18514–18517. (d) Fesko, K.; Gruber-Khadjawi, M. *ChemCatChem* **2013**, *5*, 1248–1272. (e) Alcantara, A. R.; Pace, V.; Hoyos, P.; Sandoval, M.; Holzer, W.; Hernaiz, M. J. *Curr. Top. Med. Chem.* **2015**, *14*, 2694–2711.
- (2) (a) Khalaf, J. K.; VanderVelde, D. G.; Datta, A. *J. Org. Chem.* **2008**, *73*, 5977–5984. (b) Zhang, Z.-X.; Wu, B.; Wang, B.; Li, T.-H.; Zhang, P.-F.; Guo, L.-N.; Wang, W.-J.; Zhao, W.; Wang, P. G. *Tetrahedron Lett.* **2011**, *52*, 3802–3804. (c) Mulani, S. K.; Hung, W.-C.; Ingle, A. B.; Shiau, K.-S.; Mong, K.-K. T. *Org. Biomol. Chem.* **2014**, *12*, 1184–1197.
- (3) (a) Nielsen, A. T.; Houlihan, W. J. *The Aldol Condensation. In Organic Reactions*; Wiley: New York, 2011, *16:1*, 1–438. (b) Mekelburger, H. B.; Wilcox, C. S. Formation of Enolates. In *Comprehensive Organic Synthesis*, Trost, B. M., Fleming, I., Eds; Pergamon Press: Oxford, U.K., 1991; Vol. 2, pp 99–128. (c) Heathcock, C. H. Modern enolate chemistry: regio- and stereoselective formation of enolates and the consequence of enolate configuration on subsequent reactions. In *Modern Synthetic Methods*; Scheffold, R., Ed.; Verlag Helvetica Chimica Acta: Basel, Switzerland, 1992; Vol. 6, pp 1–102. (d) Mahrwald, R., Ed. *Modern Aldol Reactions*; Springer Science+Business Media B.V.: Heidelberg, Germany, 2009.
- (4) (a) Angert, H.; Schumacher, R.; Reißig, H.-U. *Chem. Ber.* **1996**, *129*, 227–232. (b) Ghosh, A. K.; Onishi, M. *J. Am. Chem. Soc.* **1996**, *118*, 2527–2528. (c) Ghosh, A. K.; Fidanze, S.; Onishi, M.; Hussain, K. A. *Tetrahedron Lett.* **1997**, *38*, 7171–7174. (d) Ghosh, A. K.; Fidanze, S. *J. Org. Chem.* **1998**, *63*, 6146–6152. and references cited therein. (e) Koch, G.; Loiseleur, O.; Fuentes, D.; Jantsch, A.; Altmann, K.-H. *Org. Lett.* **2002**, *4*, 3811–3814. (f) Yadav, V. K.; Balamurugan, R. *Org. Lett.* **2003**, *5*, 4281–4284. (g) Ghosh, A. K.; Shevlin, M. The Development of Titanium Enolate-based Aldol Reactions. In *Modern Aldol Reactions*; Mahrwald, R., Ed.; Wiley-VCH Verlag GmbH: Weinheim, Germany, 2008; pp 63–125.
- (5) (a) Veya, P.; Cozzi, P. G.; Floriani, C.; Rotzinger, F. P.; Chiesi-Villa, A.; Rizzoli, C. *Organometallics* **1995**, *14*, 4101–4108. and cited references therein. (b) Yoshikawa, N.; Shibasaki, M. *Tetrahedron* **2001**, *57*, 2569–2579. (c) Kobayashi, S.; Saito, S.; Ueno, M.; Yamashita, Y. *Chem. Commun.* **2003**, 2016–2017. (d) Kanno, K.-I.; Takahashi, T. Zr(IV) and Hf(IV) Lewis Acids. In *Acid Catalysis in Modern Organic Synthesis*; Yamamoto, H., Ishihara, K., Eds.; Wiley-VCH Verlag GmbH&Co, KGaA: Weinheim, Germany, 2008; Vol. 2, pp 825–858.
- (6) (a) Fleming, I.; Barbero, A.; Walter, D. *Chem. Rev.* **1997**, *97*, 2063–2192. (b) Angert, H.; Czerwonka, R.; Reißig, H.-U. *Liebigs Ann./Recueil* **1997**, *1997*, 2215–2220. (c) Evans, D. A.; Burgey, C. S.; Kozłowski, M. C.; Tregay, S. W. *J. Am. Chem. Soc.* **1999**, *121*, 686–699. (d) Kobayashi, S.; Nagayama, S.; Busujima, T. *Chem. Lett.* **1999**, *28*, 71–72. (e) Mukaiyama, T.; Matsuo, J.-I. Boron and Silicon Enolates in Crossed Aldol Reaction. In *Modern Aldol Reactions*; Mahrwald, R., Ed.; Wiley-VCH Verlag GmbH: Weinheim, Germany, 2008; pp 127–161.
- (7) (a) Yanagisawa, A.; Kimura, K.; Nakatsuka, Y.; Yamamoto, H. *Synlett* **1998**, 1998, 958–960. and cited references therein. (b) Momiyama, N.; Yamamoto, H. *J. Am. Chem. Soc.* **2004**, *126*, 5360–5361. (c) Yanagisawa, A.; Yoshida, K. *Chem. Rec.* **2013**, *13*, 117–127.
- (8) (a) Donohoe, T. J. *Contemp. Org. Synth.* **1996**, *3*, 1–18. (b) Evans, D. A.; Janey, J. M.; Magomedov, N.; Tedrow, J. S. *Angew. Chem., Int. Ed.* **2001**, *40*, 1884–1888.
- (9) (a) Gennari, C.; Moresca, D.; Vulpetti, A.; Pain, G. *Tetrahedron* **1997**, *53*, 5593–5608. (b) Abiko, A.; Liu, J.-F.; Masamune, S. *J. Am. Chem. Soc.* **1997**, *119*, 2586–2587. (c) Cowden, C. J.; Paterson, I. Asymmetric Aldol Reactions Using Boron Enolates. In *Organic Reactions*; Wiley: New York, 1997; Vol. *51:1*, pp 1–200. (d) Marco, J. A.; Carda, M.; Falomir, E.; Palomo, C.; Oiarbide, M.; Ortiz, J. A.; Linden, A. *Tetrahedron Lett.* **1999**, *40*, 1065–1068. (e) Dias, L. C.; Aguilar, A. M. *Chem. Soc. Rev.* **2008**, *37*, 451–469. (f) Koskinen, A. M. *P. Chem. Rec.* **2014**, *14*, 52–61.
- (10) (a) Dénès, F.; Pérez-Luna, A.; Chemla, F. *Chem. Rev.* **2010**, *110*, 2366–2447. Aluminum enolates: (b) Loughlin, W. A.; Rowen, C. C.; McCleary, M. A. *Aust. J. Chem.* **2005**, *58*, 354–361. (c) Vuagnoux-d'Augustin, M.; Alexakis, A. *Tetrahedron Lett.* **2007**, *48*, 7408–7412. (d) Bleschke, C.; Tissot, M.; Müller, D.; Alexakis, A. *Org. Lett.* **2013**, *15*, 2152–2155. Gallium enolates: (e) Amemiya, R.; Yamaguchi, M. *Eur. J. Org. Chem.* **2005**, *2005*, 5145–5150. Indium enolates: (f) Hirashita, T.; Kinoshita, K.; Yamamura, H.; Kawai, M.; Araki, S. *J. Chem. Soc., Perkin Trans. 1* **2000**, 825–828. (g) Miura, K.; Yamada, Y.; Tomita, M.; Hosomi, A. *Synlett* **2004**, *11*, 1985–1989. (h) Baba, A.; Shibata, I. *Chem. Rec.* **2005**, *5*, 323–335. (i) Babu, S. A.; Yasuda, M.; Okabe, Y.; Shibata, I.; Baba, A. *Org. Lett.* **2006**, *8*, 3029–3032. (j) Itoh, Y.; Tsuji, H.; Yamagata, K.-I.; Endo, K.; Tanaka, I.; Nakamura, M.; Nakamura, E. *J. Am. Chem. Soc.* **2008**, *130*, 17161–17167. (k) Peppe, C.; das Chagas, R. P.; Burrow, R. A. *J. Organomet. Chem.* **2008**, *693*, 3441–3445. (l) Thirupathaiah, B.; Seo, S. Y. *Chem. Commun.* **2015**, *51*, 4216–4219.
- (11) (a) Matsumoto, K.; Ebata, T.; Koseki, K.; Kawakami, H.; Matsushita, H. *Bull. Chem. Soc. Jpn.* **1991**, *64*, 2309–2310. (b) Hung, S.-C.; Wang, C.-C.; Thopate, S. R. *Tetrahedron Lett.* **2000**, *41*, 3119–3122. (c) Lunau, N.; Meier, C. *Eur. J. Org. Chem.* **2012**, *2012*, 6260–6270.
- (12) (a) Schmittel, M.; Burghart, A.; Malisch, W.; Reising, J.; Söllner, R. *J. Org. Chem.* **1998**, *63*, 396–400. (b) Schmittel, M.; Burghart, A.; Werner, H.; Laubender, M.; Söllner, R. *J. Org. Chem.* **1999**, *64*, 3077–3085. (c) Schmittel, M.; Ghorai, M. K.; Haeusel, A.; Henn, W.; Koy, T.; Söllner, R. *Eur. J. Org. Chem.* **1999**, *1999*, 2007–2010. (d) Schmittel, M.; Ghorai, M. K. *Synlett* **2001**, *12*, 1992–1994. (e) Schmittel, M.; Haeusel, A.; Nilges, T.; Pfützer, A. *Chem. Commun.* **2003**, 34–35. (f) Haeusel, A.; Henn, W.; Schmittel, M. *Synthesis* **2003**, *16*, 2576–2589.
- (13) Huheey, J. E.; Keiter, E. A.; Keiter, R. L. *Inorganic Chemistry: Principles of Structure and Reactivity*, 4th ed.; Harper-Collins: New York, 1993.



(14) See also references cited in the following publications: Boron enolates: (a) Dias, L. C.; de Lucca, E. C.; Ferreira, M. A. B.; Garcia, D. C.; Tormena, C. F. *J. Org. Chem.* **2012**, *77*, 1765–1788. (b) Dias, L. C.; Polo, E. C.; Ferreira, M. A. B.; Tormena, C. F. *J. Org. Chem.* **2012**, *77*, 3766–3792. Titanium enolates: (c) Marrone, A.; Renzetti, A.; de Maria, P.; Gérard, S.; Sapi, J.; Fontana, A.; Re, N. *Chem. - Eur. J.* **2009**, *15*, 11537–11550. (d) Shinisha, C. B.; Sunoj, R. B. *J. Am. Chem. Soc.* **2010**, *132*, 12319–12330. (e) Sreenithya, A.; Sunoj, R. B. *Org. Lett.* **2012**, *14*, 5752–5755. (f) Renzetti, A.; Marrone, A.; Gérard, S.; Sapi, J.; Nakazawa, H.; Re, N.; Fontana, A. *Phys. Chem. Chem. Phys.* **2015**, *17*, 8964–8972. Tin enolates: (g) Blanco, O.; Pato, C.; Ruiz, M.; Ojea, V. *Org. Biomol. Chem.* **2009**, *7*, 2310–2321. (h) Ruiz, M.; Ruanova, T. M.; Blanco, O.; Núñez, F.; Pato, C.; Ojea, V. *J. Org. Chem.* **2008**, *73*, 2240–2255.

(15) (a) Lee, J. M.; Helquist, P.; Wiest, O. *J. Am. Chem. Soc.* **2012**, *134*, 14973–14981. (b) Sai, M.; Akakura, M.; Yamamoto, H. *Chem. Commun.* **2014**, *50*, 15206–15208.

(16) Indium trichloride crystallizes from THF as  $\text{InCl}_3(\text{THF})_3$ ; Wells, R. L.; Kher, S. S.; Baldwin, R. A.; White, P. S. *Polyhedron* **1994**, *13*, 2731–2735.

(17) Frisch, M. J.; Trucks, G. W.; Schlegel, H. B.; Scuseria, G. E.; Robb, M. A.; Cheeseman, J. R.; Scalmani, G.; Barone, V.; Mennucci, B.; Petersson, G. A.; Nakatsuji, H.; Caricato, M.; Li, X.; Hratchian, H. P.; Izmaylov, A. F.; Bloino, J.; Zheng, G.; Sonnenberg, J. L.; Hada, M.; Ehara, M.; Toyota, K.; Fukuda, R.; Hasegawa, J.; Ishida, M.; Nakajima, T.; Honda, Y.; Kitao, O.; Nakai, H.; Vreven, T.; Montgomery, J. A., Jr.; Peralta, J. E.; Ogliaro, F.; Bearpark, M.; Heyd, J. J.; Brothers, E.; Kudin, K. N.; Staroverov, V. N.; Kobayashi, R.; Normand, J.; Raghavachari, K.; Rendell, A.; Burant, J. C.; Iyengar, S. S.; Tomasi, J.; Cossi, M.; Rega, N.; Millam, J. M.; Klene, M.; Knox, J. E.; Cross, J. B.; Bakken, V.; Adamo, C.; Jaramillo, J.; Gomperts, R.; Stratmann, R. E.; Yazyev, O.; Austin, A. J.; Cammi, R.; Pomelli, C.; Ochterski, J. W.; Martin, R. L.; Morokuma, K.; Zakrzewski, V. G.; Voth, G. A.; Salvador, P.; Dannenberg, J. J.; Dapprich, S.; Daniels, A. D.; Farkas, Ö.; Foresman, J. B.; Ortiz, J. V.; Cioslowski, J.; Fox, D. J. *Gaussian 09*, Revision D.01; Gaussian, Inc.: Wallingford, CT, 2010.

(18) (a) Becke, A. D. *J. Chem. Phys.* **1993**, *98*, 1372–1377. (b) Becke, A. D. *J. Chem. Phys.* **1993**, *98*, 5648–5652.

(19) Lee, C.; Yang, W.; Parr, R. G. *Phys. Rev. B: Condens. Matter Mater. Phys.* **1988**, *37*, 785–789.

(20) (a) Hay, P. J.; Wadt, W. R. *J. Chem. Phys.* **1985**, *82*, 270–283. (b) Wadt, W. R.; Hay, P. J. *J. Chem. Phys.* **1985**, *82*, 284–298. (c) Hay, P. J.; Wadt, W. R. *J. Chem. Phys.* **1985**, *82*, 299–310.

(21) Swiss, K. A.; Choi, W. B.; Liotta, D. C.; Abdel-Magid, A. F.; Maryanoff, C. A. *J. Org. Chem.* **1991**, *56*, 5978–5980.